AGU ADVANCING EARTH AND SPACE SCIENCE

Water Resources Research

RESEARCH ARTICLE
10.1029/2020WR029314

The Long-Term Response of Alternate Bars to the Hydrological Regime

Mattia Carlin[1], **Marco Redolfi**[1], **and Marco Tubino**[1]

[1]Department of Civil, Environmental and Mechanical Engineering, University of Trento, Trento, Italy

Key Points:

- We propose a theoretically based method for predicting the long-term response of migrating bars to the hydrological regime
- Our procedure allows for determining whether alternate bars are expected to form, and for predicting their average height
- We define a bar-forming discharge that, if applied steadily, would produce the same morphology as the full hydrological regime

Supporting Information:

Supporting Information may be found in the online version of this article.

Correspondence to:

M. Carlin,
mattia.carlin@unitn.it

Citation:

Carlin, M., Redolfi, M., & Tubino, M. (2021). The long-term response of alternate bars to the hydrological regime. *Water Resources Research*, *57*, e2020WR029314. https://doi.org/10.1029/2020WR029314

Received 28 NOV 2020
Accepted 26 JUN 2021

Abstract Migrating bars are large-scale, alternate bedforms that often develop in channelized river reaches, as a consequence of an intrinsic instability of the erodible channel bed. Their behavior under steady flow conditions has been widely investigated by means of theoretical, experimental, and numerical models, which revealed that bar formation occurs when the width-to-depth ratio of the channel exceeds a critical threshold value. Conversely, no much information is available about the long-term, average characteristics of alternate bars in the case of a complex flow regime, which makes the width-to-depth ratio highly variable in time. Starting from the state-of-the-art theoretical models of bar dynamics, we propose a novel methodology to determine the long-term bar response to the hydrological river regime and the associated "bar-forming" discharge that, if applied steadily, would produce the same morphological response. We derive a generalized criterion to define whether bars are expected to form and to estimate the long-term bar topography, depending on flow probability density function and channel characteristics (width, slope and sediment size). Our procedure differs from the classical methods to define formative discharge, inasmuch as it accounts for the specific and reversible response of bar topography to the different flow stages that compose the hydrological regime. Application to four different gravel bed reaches in the Alpine region shows the capability of the procedure to interpret remarkably different riverbed morphologies and to provide a reasonable prediction of the observed bar height, thus suggesting its potential to analyze long-term morphological trajectories following hydrological alterations and river restoration projects.

Plain Language Summary Alternate bars are large bedforms that can spontaneously develop in rivers. They often represent an issue in river management since they affect navigation, increase the flooding risk and interact with instream structures. A number of studies is available to predict the characteristics of alternate bars under constant-discharge conditions. Conversely, the long-term response of the average bar topography to a complex sequence of flood events is to a large extent unexplored. In this work, we propose a novel theoretically based procedure to assess whether alternate bars are expected to form in a river, to predict the average bar height, and to estimate the equivalent, bar-forming discharge that can be effectively used in constant-discharge models. This method may be used for evaluating the response of alternate bars to modifications of the hydrological flow regime (e.g., due to climate changes or hydropower production) or river restoration interventions (e.g., enlargement or narrowing of the channel width).

1. Introduction

In the last few centuries, many European rivers were regulated to increase land availability and industry production, and to reduce the flooding risk (Dynesius & Nilsson, 1994; Molle, 2009; Nilsson et al., 2005). In particular, their course was often straightened and their width was typically restricted by the construction of embankments (Diaz-Redondo et al., 2017; Hohensinner et al., 2007; Scorpio et al., 2018; Serlet et al., 2018). Despite the very regular geometry that was artificially imposed, the riverbed often reacted by self-producing a sequence of scour and deposition zones, typically migrating downstream, called alternate bars. Due to their relatively high relief and their capability to modify the riverbed pattern, alternate bars may affect channel navigability and interact with structures, and therefore their occurrence represents one of the most problematic aspects in the management of regulated rivers.

As widely documented by theoretical, numerical, and laboratory investigations (e.g., Crosato et al., 2011; Defina, 2003; Fredsoe, 1978; Ikeda, 1984; Jaeggi, 1984; Lanzoni, 2000; Nelson, 1990; Parker, 1976; Qian

et al., 2017), migrating alternate bars spontaneously develop in straight channels due to a riverbed instability mechanism, which occurs when the channel width-to-depth ratio exceeds a threshold value. Under constant discharge conditions, alternate bars grow until they attain a regime state, where they maintain the same average properties (height, wavelength, and shape) while migrating downstream, although long-term fluctuations are possible (Crosato et al., 2012). Conversely, under unsteady flow conditions alternate bars evolve by varying their morphometric properties depending on the intensity and duration of flood events (e.g., Eekhout et al., 2013; Hall, 2004; Tubino, 1991; Welford, 1994).

For given river geometry, the threshold condition for bar formation corresponds to a specific discharge value, and therefore the hydrological regime may include, in general, both bar-forming and bar-suppressing stages. Existing studies on bar response to variable discharge (Adami et al., 2016; Jaballah et al., 2015; Jourdain et al., 2020; Nelson & Morgan, 2018) mainly focused on the effect of individual flow events, and therefore no much information exists about the expected properties of alternate bars as a result of the complex sequence of events that characterize the hydrological regime. The question then arises of how to define a criterion to determine how likely alternate bars are to be present in a river reach and to predict their long-term average properties, or alternatively, a "bar-forming" discharge value associated to such average conditions.

Defining the average response of a river reach to the hydrological regime and identifying a suitable metric (a specific discharge value) that controls such response are very common issues in river morphodynamics. To address these issues, the concept of "formative" or "dominant" discharge was first introduced by Inglis (1949), as the discharge value that produces the same effect on river morphology as the whole hydrological series. Since then, various methods have been proposed in the literature (see Blom et al., 2017) to define the formative conditions for specific river properties (e.g., channel width, longitudinal slope, bed surface texture), such as the bankfull discharge (Andrews, 1980; Emmett & Wolman, 2001; Inglis, 1949; Leopold & Wolman, 1957) or the discharge value associated to a fixed (1.5–2 year flood) recurrence interval (see Nash, 1994; Pickup & Warner, 1976; Williams, 1978, for example). Among them, the "effective discharge" concept proposed by Wolman and Miller (1960) has been widely used to describe phenomena in which the solid transport is the main driver of morphological evolution (Andrews, 1980; Benson & Thomas, 1966). The method considers as "dominant" the discharge that moves the largest volume of sediments over a period of time. It combines the magnitude of the hydrological events with their frequency of occurrence, taking the product between the duration curve of the flow series and the solid transport rate, which is commonly modeled by deterministic transport predictors. The effective discharge method has been extensively employed in the case of sandy streams, due to easier availability of sediment transport data (i.e., Ashmore & Day, 1988; Benson & Thomas, 1966; Crowder & Knapp, 2005; Ferro & Porto, 2012). However, many applications to gravel bed rivers are also documented in the literature, both using theoretical bedload predictors (Andrews, 1980; Barry et al., 2008; Pickup & Warner, 1976) and field data (Carling, 1988; Downs et al., 2016; Emmett & Wolman, 2001; Goodwin, 2004). In the case of coarse and natural rivers, predicted formative values are in fairly good agreement with those obtained with the alternative definitions of bankfull discharge or 1.5–2 year flood (Andrews, 1980; Doyle et al., 2007; Emmett & Wolman, 2001), while they substantially differ in regulated-channelized rivers (Doyle et al., 2007) and flashy systems (Pickup & Warner, 1976).

Despite the various attempts to define a generally valid concept of formative discharge, it clearly appears that its definition needs to be related to the specific morphodynamic aspect under investigation (e.g., Church & Ferguson, 2015), as "no single steady discharge can affect all characteristics of channel geometry in a similar manner as the varying flow rate" (Blom et al., 2017). Furthermore, other variables affect the morphodynamical response of rivers to the hydrological regime, such as the catchment area, the climate characteristics of the region, the nature of sediment transport and the river pattern. For example, small basins tend to be controlled by catastrophic events (Ashmore & Day, 1988), even more so when they are located in semi-arid regions (Baker, 1977; Selby, 1974), and the formative processes that govern channel morphology are different in the case of braided rivers (Surian et al., 2009) or mountain streams (Vianello & D'Agostino, 2007).

Why do we need a novel, specific approach to determine the long-term average bar response to the hydrological regime? Indeed, the effective discharge method implies four main assumptions: (a) the morphodynamical work increases with the sediment transport, and therefore with flow discharge; (b) increasing the

flow discharge, the timescale of bed evolution gets shorter according to the Exner equation, and therefore the river response gets faster; (c) all the flow stages above the threshold of incipient sediment motion work in the same direction, their effect increasing monotonically with flow discharge; (d) the response of sediment transport to flow variability is instantaneous. None of these assumptions perfectly fit the observed behavior of alternate bars. As discharge increases, the width-to-depth ratio decreases and so does the equilibrium amplitude of bars (Redolfi et al., 2020). Moreover, the growth rate of bars (that is the reciprocal of the timescale) increases to a maximum value and then drops at higher discharge, until it becomes negative. This sets a second, upper threshold (the critical discharge for bar formation) that discriminates bar-forming from bar-suppressing flow stages: the fact that the morphodynamical work acted on river bars by relatively low-flow stages can be reversed by high-flow stages ultimately represents the key difference with respect to other river properties. Finally, the time scale of bar amplification/decay is often comparable with that associated with flood events. Therefore, bar adaptation to flow variability is not instantaneous (Tubino, 1991; Welford, 1994), which implies that bar height may not attain at each flow stage the corresponding equilibrium value.

The need for a specific representative discharge for alternate bars have been already highlighted by Jaballah et al. (2015), while Crosato and Mosselman (2009), in the absence of a suitable estimate, used the bankfull discharge to define a criterion for the occurrence of bars. Such need is also supported by the few available field observations, which suggest that bar topography is mainly determined by specific flow conditions, such as the tails of flow hydrographs (Welford, 1994) or the "bar-full" stage (Biedenharn & Thorne, 1994).

In this work, we propose a new method to define an occurrence criterion for alternate bars in channelized river reaches that accounts for the hydrological regime. We then derive an estimate of the bar-forming discharge, defined as the discharge whose corresponding bar height coincides with the average value resulting from the hydrological cycle. The method is based on the statistical distribution of flow events and on the response of free alternate bars obtained from the weakly nonlinear Colombini et al. (1987) model. The occurrence criterion and the bar-forming discharge arise from a balance between bar-forming and bar-suppressing flow stages, which represents the key novelty of our approach with respect to the classical concept of effective discharge. The procedure has been applied to different gravel bed river reaches, the Alpine Rhine River (Switzerland), the Isère River (France), and the Adige River (Italy), for which long flow records were available, each of them characterized by a distinctive average bed response.

The manuscript is organized as follows. In Section 2 we briefly summarize previous experimental and theoretical results on free alternate bars, highlighting their dependence on flow discharge. A general description of the study cases is proposed in Section 3. The new model is formulated in Section 4 and applied to four selected study cases in Section 5. In Section 6 we discuss the main implications and limitations of the proposed approach; finally, we draw some conclusions in Section 7.

2. The Response of Alternate Bars to Discharge Variations

The formation of migrating bars is one of the most studied topics in river morphodynamics. The large number of laboratory observations, numerical, and theoretical results produced so far provides a consistent picture of the dependence of bar properties (morphology, migration rate) on flow and sediment characteristics and highlights the role of the channel aspect ratio β, defined as the ratio between the half-width and the average flow depth, as the main controlling parameter of bar instability (e.g., Bertagni & Camporeale, 2018; Colombini et al., 1987; Fredsoe, 1978; Siviglia et al., 2013; Tubino et al., 1999).

On one hand, the free development of alternate bars depends on the aspect ratio being smaller or larger than a critical threshold β_{cr}: in relatively narrow channels (subcritical region) the stabilizing effect of transverse bed load transport prevents the formation of alternate bars, while in wider channels this effect gets weaker and alternate bars spontaneously form. On the other hand, the equilibrium bar height, increases as β departs from the critical threshold, that is, with $(\beta - \beta_{cr})$. The region of bar instability enlarges (i.e., β_{cr} gets smaller) as the Shields parameter approaches the condition of incipient sediment motion as well as for increasing values of the relative grain roughness.

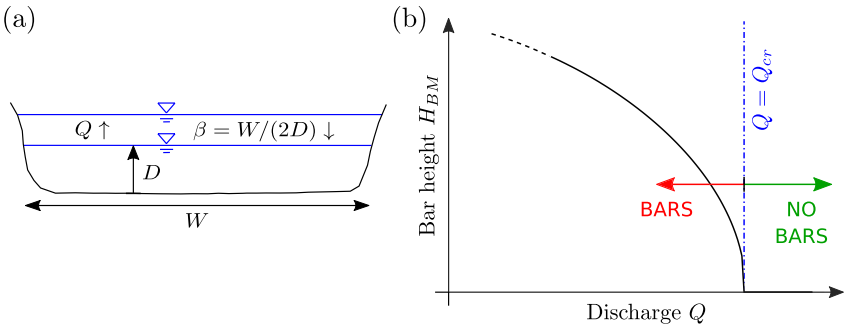

Figure 1. Equilibrium response of alternate bars to discharge variations: (a) the effect of increasing discharge, which leads to a decrease of the channel aspect ratio β; (b) the dependence of equilibrium bar height on flow discharge resulting from the Colombini et al. (1987) weakly nonlinear theory.

In single thread channels, both the critical threshold and the actual value of the aspect ratio significantly change with water discharge. Specifically, being β inversely proportional to water depth, its value typically decreases with increasing flow discharge, as sketched in Figure 1a, and so does the equilibrium bar height. The dependence of bar height on flow discharge for a given river reach, as predicted by the weakly nonlinear theory of Colombini et al. (1987), is shown in Figure 1b, where H_{BM} denotes the difference between the maximum and minimum bed elevation within a bar unit. Once inspected in terms of discharge variations, theoretical results also allow for defining a critical threshold discharge for free bars formation, Q_{cr}, as the value at which the condition $\beta = \beta_{\mathrm{cr}}$ is met (see Redolfi et al., 2020).

Such decreasing trend of bar height with flow discharge is confirmed by the reanalysis of existing laboratory experiments with relatively coarse bed material, as reported in Figure 2. We considered the experiments of Kinoshita (1961), Sukegawa (1971), Jäggi (1983), and Redolfi et al. (2020), which include data on equilibrium bar properties for different values of discharge, channel width, channel slope and sediment size. These data were processed as follows: we grouped experiments having the same channel width and sediment size, and a similar slope, with maximum deviation from the median value of 20% (each group is represented in Figure 2 with a different marker); we only considered groups that encompassed at least three distinct discharge values. Furthermore, discharge was expressed per unit channel width W, and made dimensionless as in Parker et al. (2007):

$$q^{*} = \frac{Q}{W\sqrt{g d_{50}^{3}}}, \tag{1}$$

where g is the gravitational acceleration and d_{50} is the median grain size. For almost all groups of experiments reported in Figure 2, a relatively sharp decline of bar height with flow discharge is displayed, which closely resembles that reported in Figure 1b. Hence, both theoretical results and experimental findings clearly highlight a first distinctive characteristic of free alternate bars: their amplitude inversely depends on the water discharge.

A second, specific aspect that characterizes the response of river bars to different flow stages is the rate of change of their amplitude, which is defined as:

$$\Omega := \frac{1}{A}\frac{dA}{dt}, \tag{2}$$

where the generic symbol A is used here to encompass the various metrics proposed in the literature to measure the bar height (see Redolfi et al., 2020, for a review of the main metrics). One can readily recognize that Ω is the reciprocal of the time scale of the process, and therefore represents a key ingredient to determine the effectiveness of a given flow stage to produce a morphodynamical response.

In general terms, the speed of riverbed evolutionary processes is set by the Exner continuity equation, and therefore it increases with sediment transport intensity, whence with flow discharge. However, bar

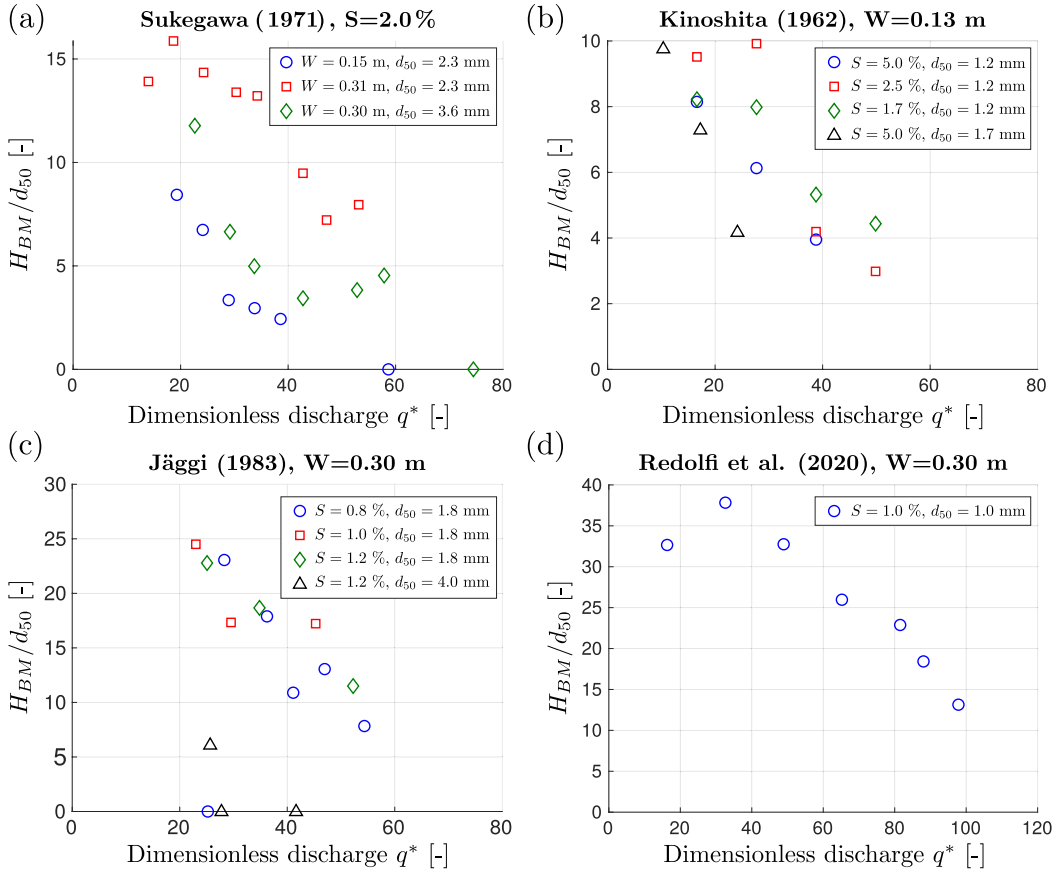

Figure 2. Relationship between the equilibrium bar height and the unit discharge resulting from the laboratory experiments of Kinoshita (1961), Sukegawa (1971), Jäggi (1983), and Redolfi et al. (2020), which cover a wide range of conditions in terms of channel width (W), average downstream slope (S) and median grain size (d_{50}). To make the different experiments comparable, bar height is scaled with the grain size (H_{BM}/d_{50}) and discharge is made dimensionless according to Equation 1.

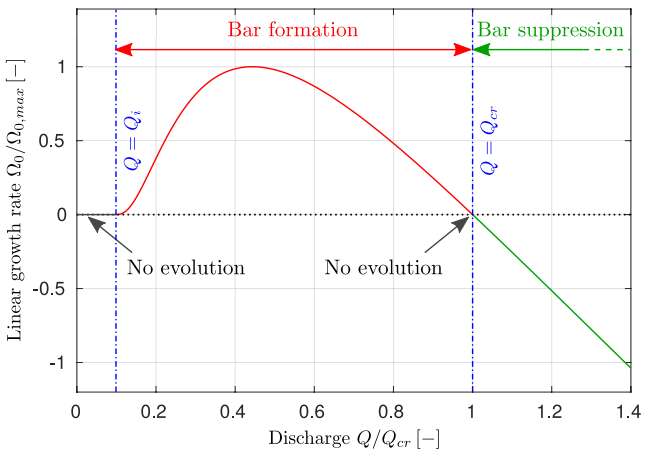

Figure 3. The linear growth rate of free alternate bars, scaled with its maximum value $\Omega_{0,max}$, as a function of water discharge. The critical threshold Q_{cr} discriminates between bar-forming ($\Omega_0 > 0$) and bar-suppressing ($\Omega_0 < 0$) flow conditions. When discharge is lower than the threshold of incipient sediment motion, Q_i, the growth rate vanishes and bar evolution is inhibited.

instability exhibits a remarkably different behavior, as shown in Figure 3 where we report an example of the dependence of the growth rate of alternate bars on flow discharge resulting from linear bar theories (the subscript "0" denotes the linear value of the growth rate) (e.g., Federici & Seminara, 2006; Fredsoe, 1978). We note that the growth rate vanishes at two distinct discharge conditions: (a) near the threshold of incipient sediment motion (i.e., $Q = Q_i$), where the sediment transport is so low that no morphological activity is possible; (b) near the critical conditions for bar formation (i.e., $Q = Q_{cr}$), where the tendency to form alternate bars becomes very weak. While the first threshold appears in most river morphodynamic processes, the second is a distinctive characteristic of free alternate bars, which originates from their instability mechanisms. Furthermore, the bar growth rate becomes negative when Q exceeds Q_{cr}, which implies that high flow stages may counteract the bar-forming effect exerted by lower stages.

It is worth noticing that the linear estimate of the bar growth rate is suitable to describe the expected tendency of a given flow stage to form (or suppress) migrating river bars provided their amplitude is small, strictly infinitesimal. In actual situations, flood events are likely to rework an already existing bar topography, which requires also to account for finite

amplitude effects on bar growth. In Section 4, we discuss how the scenario depicted in Figure 3 changes when the weakly nonlinear estimate of Colombini et al. (1987) for the growth rate is adopted.

The above description of bar response to variable flow discharge can be readily extended to higher order transverse modes (i.e., central or multiple-row bars). Their critical threshold (say, for mode m) is related to β_{cr} through the relationship $\beta_{cr,\,m} = m\beta_{cr}$, and therefore higher-order modes require large values of width-to-depth ratio to form, the corresponding values of the critical discharge being much smaller than Q_{cr}. However, in relatively wide channels favorable conditions for their growth can be frequently encountered at low flow stages that are still capable of transporting sediment (e.g., Rodrigues et al., 2015). In the following sections, we will focus our attention on the alternate bars mode $m = 1$. However, we will discuss about the limitations and potential extension of our approach to higher-order modes at the end of Section 6.

3. Study Reaches

In this work, we have investigated the riverbed response to the hydrological regime of four study reaches located in three rivers of the alpine region whose flow regime is markedly regulated: the Alpine Rhine River, the Isère River, and the Adige River. All these reaches are channelized and only weakly curved. Figure 4 shows a planform view of the study reaches, whose lengths range from 5 to 15 km, while Table 1 summarizes the reach-averaged values of river properties, as adopted in our analysis, as well as the relevant morphological and hydrological information. Reported values of channel width refer to the morphodynamically active part of the river section, which has been taken to coincide with the bottom width.

The Rhine River, with a catchment area of about 190,000 km^2 and a length of 1326 km is one of the largest rivers in Europe, flowing from the Swiss Alps to the North Sea. The first 93 km of the river, from the confluence between Vorderrhein and Hinterrhein and the Lake of Constance, form the so-called Alpine Rhine. The Alpine subbasin of the Rhine River covers the whole territory of Liechtenstein, the western part of Austria and the eastern part of Switzerland, draining an area of 6,123 km^2. In the 19th and 20th century, the Alpine Rhine River was heavily channelized, drastically simplifying the complex multithread morphology (Adami et al., 2016). We have focused our analysis on two reaches located upstream and downstream the confluence of the Ill River (located near Eichenwies), which are representative of two different morphological responses of the riverbed to channelization. In particular, as shown in Figure 4a, the wider upstream reach presents a continuous sequence of alternate bars, while the narrower downstream reach displays a simpler morphology without evident bedforms. For this reason, the Alpine Rhine River can be considered an optimal morphodynamic laboratory, where two opposite bed responses manifest themselves, despite the very similar hydrological and sedimentological conditions. The flow regime is pluvio-nival, with significant snowmelt in spring and summer and larger floods mainly in autumn. Discharge data recorded at intervals of 10 min are available from the Swiss station of Diepoldsau from 1984 to 2010.

The Isère River is 286 km long, flowing from the Graian Alps of Savoia (south-eastern France) to the Rhône River near Valence. The catchment area is about 12,000 km^2. In the 19th century the river was channelized and straightened, causing the modification of riverbed morphology from braided to single-thread with alternate bars (Serlet et al., 2018). After the channelization, an intensive exploitation of the river basin resources for hydropower production began, with the construction of several dams in the early 20th century and two interbasin transfers. Our study reach is located near Montmèlian, downstream the confluence of the Arc River. The human pressures have strongly impacted on the natural nivo-glacial flow regime and the sediment supply, determining nowadays a very stable sequence of bars, mostly vegetated (see Serlet et al., 2018), as shown in Figure 4b. Hourly discharge data are available for the Montmèlian station from 1988 to 2015.

The Adige River, with a catchment of about 12,200 km^2 and an approximate length of 410 km, is the second longest river in Italy, flowing from the central-eastern Alps to the Adriatic Sea. Some works on channel bank stabilization have been carried out since the Middle Age, while a strong channelization was realized in the 19th century. Our study reach is near the city of Trento, where the channel has a bottom width of about 70 m. Sediment samples collected at low flow stages in a recent field survey (Scorpio et al., 2018) have highlighted the presence of a pronounced armoring that is likely to persist over typical floods (Wilcock & DeTemple, 2005). A surface-based estimate provides a value of the median grain size of 53 mm. The bed morphology of the whole channelized part of the river is almost flat, without river bedforms (see Scorpio

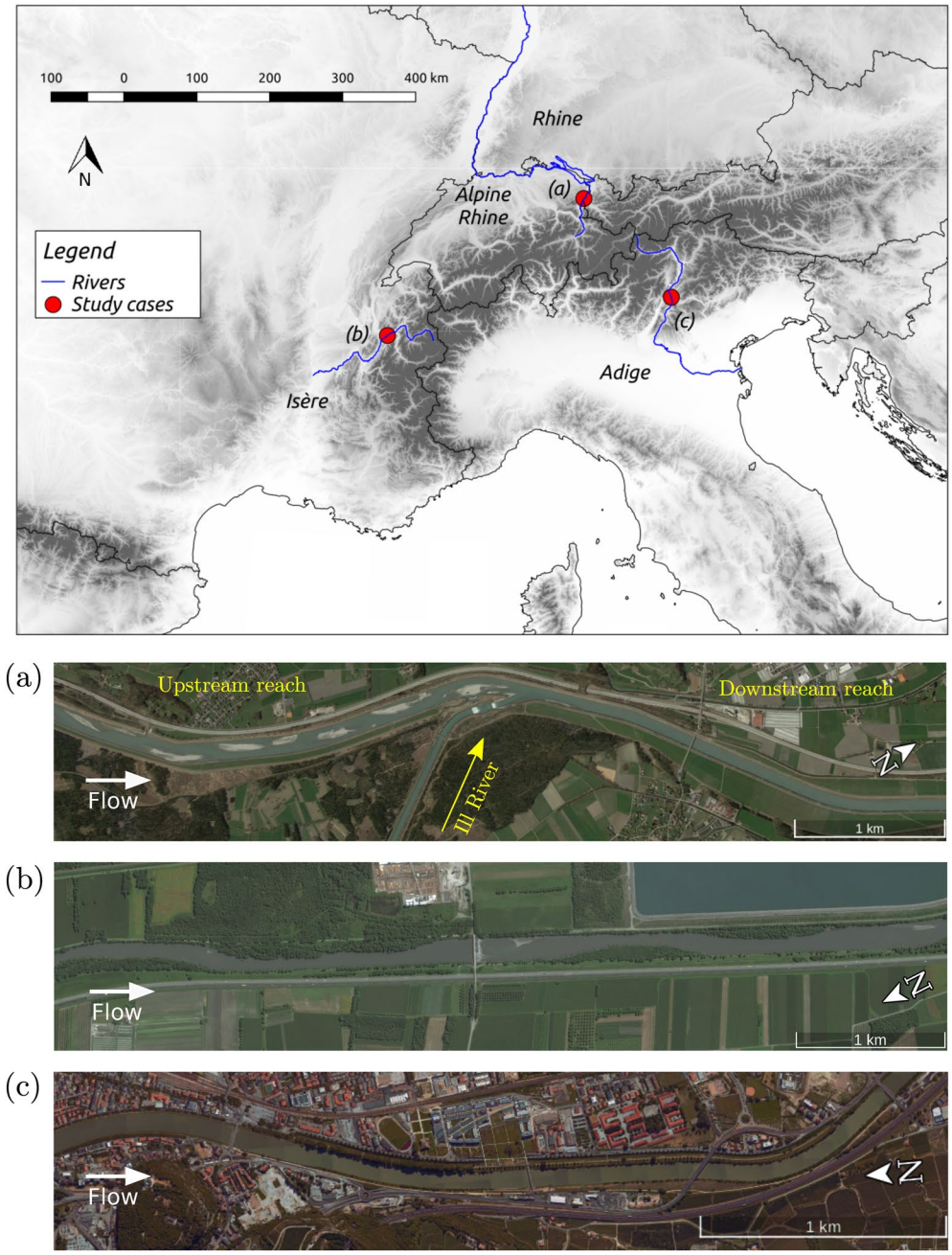

Figure 4. Location of the study cases in the alpine region. (a) Two reaches of the Alpine Rhine River, upstream and downstream the confluence of the Ill River, showing a transition from a clear alternate bar pattern to no evident bedforms; 09-Jul-2016, 47°17′N, 09°33′E; (b) Isère River with stable, vegetated bars, 28-Aug-2014, 45°23′N, 05°59′E; (c) Adige River with a flat bed morphology, 19-Jul-2015, 46°03′ N, 11°06′E. From Google Earth, Digital Globe (2019).

et al., 2018), as shown in Figure 4c. The original flow regime was nivo-glacial, characterized by the minimum flow in winter and larger floods in autumn due to long-lasting cyclonic fronts. Nowadays, the Adige River basin is one of the most exploited in Italy for hydropower production, with a large number of dams built along its tributaries, which have heavily modified the flow regime and filtered the sediment supply. Discharge data recorded at intervals of 30 min are available for the gauging station of Trento-San Lorenzo from June 1994.

Table 1
Summary of Data for the Four Study Reaches, With the Respective References. $\bar{Q}$ and Q_{max} Indicate the Mean and the Maximum Discharge, Q_2 is the Discharge Having a Return Period of Two Years and c_v is the Coefficient of Variation (i.e., the Ratio Between the Standard Deviation and the Mean) of the Entire Flow Series

	Alpine Rhine[a]			
	Upstream	Downstream	Isère[b]	Adige[c]
Geometry				
Channel slope (%)	0.13	0.10	0.19	0.08
Channel width (m)	106	63	92	70
Median grain size (mm)	25	25	35	53
Flow regime				
$\bar{Q}$ (m^3s^{-1})	166	231	121	205
Q_2 (m^3s^{-1})	1075	1231	463	754
Q_{max} (m^3s^{-1})	2399	2666	791	1885
c_v (-)	0.74	0.68	0.53	0.61
Bar morphology	High-relief bars	Low-relief bars	Vegetated bars	No bars

[a]Adami et al. (2016), Mähr et al. (2014). [b]Vautier (2000). [c]Scorpio et al. (2018).

4. A Method to Determine the Response of Alternate Bars to the Hydrological Forcing

In this section, we introduce a novel methodology to evaluate the long-term bar response to the river hydrograph, accounting for the key factors that characterize the response of bars to variations of flow discharge. We employ the case of the Alpine Rhine River, where two consecutive reaches exhibit similar hydrological and sedimentological characteristics, but a different bed configuration, as an optimal example to illustrate our procedure and to highlight the difference with respect to the classical method of the effective discharge (Wolman & Miller, 1960).

We assume a rectangular cross section and we compute uniform-flow parameters (i.e., water depth, velocity, and associated dimensionless parameters) at different levels of discharge by considering the Engelund and Fredsoe (1982) friction formula. Moreover, we estimate the sediment rating curve through the Parker (1978) transport formula, assuming a relative submerged weight of sediment $\Delta = 1.65$. Sensitivity of model results to the adopted transport predictor is tested in Section 5, where Meyer-Peter and Muller (1948) formula is also employed. The linear growth rate and the equilibrium amplitude of bars are evaluated through the analytical model of Colombini et al. (1987), where the empirical coefficient r that measures the effect of gravity on transverse transport has been set equal to 0.6.

To introduce our procedure, we first consider the application of the effective discharge method to the "upstream" reach of the Alpine Rhine River as reported in Figures 5a and 5b: the effective discharge, around $Q = 405\ m^3\ s^{-1}$, is calculated as the peak value of the product between the flow probability density function, f_Q, and the sediment rating curve, $Q_s(Q)$. The significance of this value is clear: it represents the discharge that on average gives the maximum contribution to the annual sediment transport (for details, see supporting information).

A complementary interpretation of the geomorphic significance of the above procedure can be obtained by considering that the morphodynamical efficacy of each flow stage, which is assumed to increase proportionally with the sediment transport rate, can be equivalently defined in terms of the timescale of the evolutionary process. Specifically, the timescale of the associated geomorphic changes, T_{exn}, can be estimated by means of the Exner continuity equation, which gives an inversely proportional relation with the sediment transport rate Q_s:

$$T_{exn} \propto 1 / Q_s. \tag{3}$$

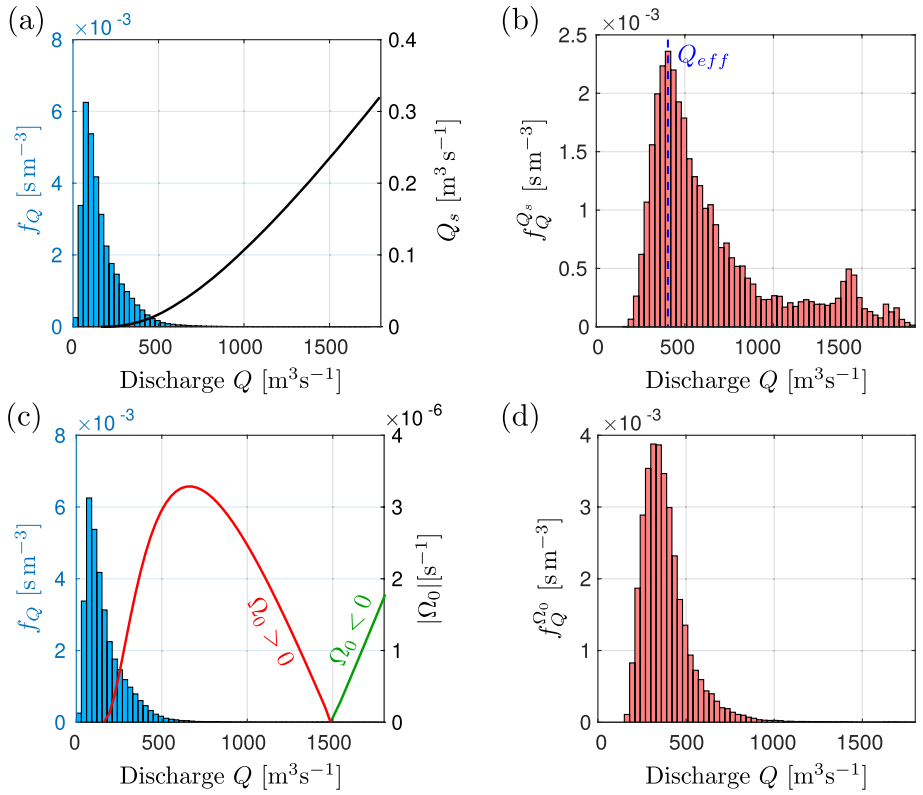

Figure 5. (a, b) The method of Wolman and Miller (1960) applied to the Rhine River reach upstream of the confluence of the Ill River. The effective discharge, Q_{eff}, corresponds to the peak of $f_Q^{Q_s}$ (b), which is obtained by multiplying (a) the flow probability density function, f_Q, by the sediment rating curve, $Q_s(Q)$. (c, d) For the same river reach, the probability density function of flow stages, scaled with the timescale of bar adaptation, $f_Q^{\Omega_0}$ (d), which is obtained by multiplying (c) the flow probability density function, f_Q, by the absolute value of the linear growth rate, Ω_0.

We then express the time in terms of T_{exn} units, defining a dimensionless time, t^*, whose increments are defined as:

$$dt^* = dt \,/\, T_{exn}. \tag{4}$$

Plotting the flow series as a function of t^* gives a reshaped hydrograph $Q(t^*)$, whose probability density function can be calculated as follows:

$$f_Q^{Q_s} = \frac{f_Q Q_s}{\int_0^\infty f_Q Q_s \, dQ}, \tag{5}$$

which coincides with the definition proposed by Blom et al. (2017) in their Equation 35. The scaled probability density function (Equation 5) provides a different interpretation of the effective discharge value as the most frequent flow state in the "*time of the sediment transport*."

4.1. A Criterion for the Alternate Bars Formation

To apply a similar concept to the case of alternate bars, it is crucial to consider that the speed of bar adaptation is not simply proportional to the sediment transport rate, but it rather depends on the growth rate (here we consider the linear value Ω_0). Therefore, it follows the nonmonotonic curve represented in Figure 3, which vanishes at both the threshold for incipient sediment motion and at the critical threshold for bar formation. Hence, we define the timescale of bar response as follows:

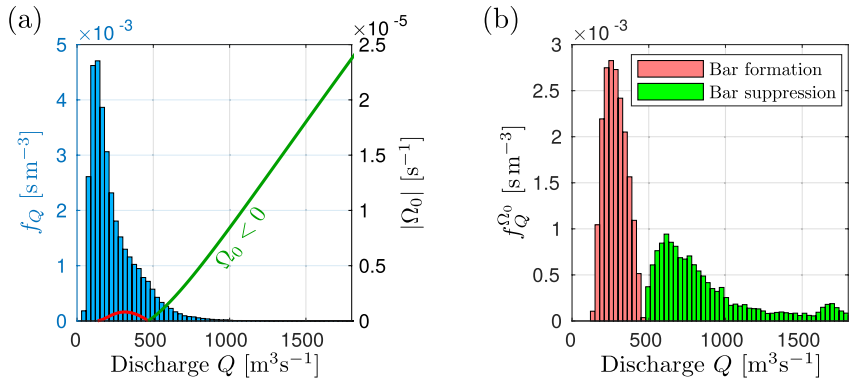

Figure 6. The Rhine River reach downstream of the confluence of the Ill River: the probability density function of flow stages, scaled with the timescale of bar adaptation, $f_Q^{\Omega_0}$ (b), which is obtained by multiplying (a) the flow probability density function, f_Q, by the absolute value of the linear bar growth rate, $|\Omega_0|$. Colors identify bar-forming ($\Omega_0 > 0$) or bar-suppressing ($\Omega_0 < 0$) flow stages, depending on discharge being lower or higher than the critical threshold Q_{cr}.

$$T_{bars} = 1 / \left|\Omega_0\right|. \tag{6}$$

Scaling the time with T_{bars}, we then obtain a reshaped hydrograph that is associated with the following probability density function:

$$f_Q^{\Omega_0} = \frac{f_Q \left|\Omega_0\right|}{\int_0^\infty f_Q \left|\Omega_0\right| dQ}, \tag{7}$$

which represents the probability of observing a given discharge Q in the "*time of bar adaptation*." Therefore, $f_Q^{\Omega_0}(Q)$ indicates the effectiveness of each discharge state in forming ($\Omega_0 > 0$) or suppressing ($\Omega_0 < 0$) alternate bars.

As illustrated in Figures 5c and 5d, this probability is basically obtained as the (scaled) product between the flow probability density function, f_Q, and the linear growth rate of bars, Ω_0. Similar to the approach of Wolman and Miller (1960), in this case the peak of the histogram gives the value of discharge that is more effective in forming bars, which turns out to be slightly lower than the effective discharge value of Figure 5b.

We note that in the case of the upstream reach of the Rhine River the predicted critical discharge value for bar formation is quite large, approximately $Q_{cr} = 1500$ m^3 s^{-1}, and therefore the contribution of the extremely rare bar-suppressing stages ($\Omega_0 < 0$) is not appreciable. In other words, within this reach bar formation is enhanced at almost all flow stages above the threshold for sediment motion Q_i. Under these circumstances, the information obtained through Equation 7 does not differ substantially from that resulting from the effective discharge method, but for the shift of the peak discharge toward lower values.

The difference between the two approaches becomes more evident when applying the same procedure to the downstream reach of the Alpine Rhine River, for which the predicted critical discharge for bar formation is much smaller, approximately $Q_{cr} = 467$ m^3 s^{-1}, and then the product of the probability density function and the linear growth rate provides the bi-modal distribution reported in Figure 6b. The two peaks still identify two discharge values of maximum effectiveness; however, their meaning is different, as events with $Q < Q_{cr}$ work to form the bars, while events with $Q > Q_{cr}$ work to suppress them. Hence, Figure 6 highlights the important consequence of bars being a threshold process: different discharge states are not only characterized by different effectiveness, but they also work in opposite (i.e., bar forming vs. bar suppressing) directions, as also previously suggested by Adami et al. (2016). Even though the slight preeminence of the red area suggests that bar-forming flow events tend to prevail in the downstream reach, we expect the height of bars to be much smaller than that in the upstream reach.

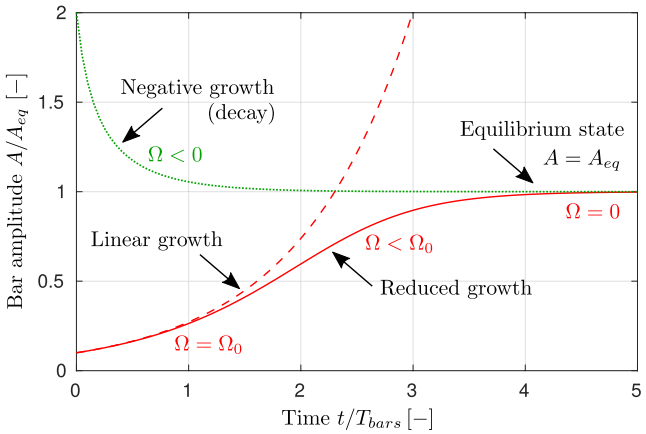

Figure 7. Evolutionary trajectories of bar amplitude, scaled by its equilibrium value A_{eq}, for a steady discharge $Q < Q_{cr}$ (i.e., under bar-forming conditions), as predicted by the weakly nonlinear theory of Colombini et al. (1987). When $A \ll A_{eq}$ bar amplitude increases according to the linear growth rate Ω_0 (dashed line), while the growth rate gradually decreases when the amplitude approaches its equilibrium value. If $A > A_{eq}$ the growth rate is negative, and then bars tend to return to their equilibrium state. Time is scaled with the characteristic time of bar growth defined in Equation 6.

The recognition that bar topography can be continuously reworked by the counteracting effect of different flow stages suggests that the average bar response to the hydrological cycle, rather than being associated to a most effective discharge value, ultimately results from the cumulative effect of the entire range of discharge states. Specifically, it depends on the competition between bar-forming and bar-suppressing events, whose overall effectiveness can be measured by the area of the histogram $f_Q^{\Omega_0}$, which represents a probability. We then define the probability of bar formation in the following form:

$$P_{form} = P_0(Q < Q_{cr}) = \int_0^{Q_{cr}} f_Q^{\Omega_0}\, dQ, \tag{8}$$

while its complement, $1 - P_{form}$, represents the probability of bars to be suppressed. Therefore, an occurrence criterion for alternate bars that accounts for the hydrological regime can be obtained in the following simple form:

$$P_{form} > 0.5, \tag{9}$$

which also corresponds to the condition that the mean growth rate is positive, namely:

$$\bar{\Omega}_0 = \int_0^{\infty} \Omega_0 f_Q\, dQ > 0. \tag{10}$$

The above criterion is obviously not strict, as different sources of uncertainties exist in the evaluation of lower and upper threshold discharges, Q_i and Q_{cr}. Furthermore, it refers to the average state, and therefore indicates a preference for a particular morphodynamic style. Specifically, the probability P_{form} provides a measure of "*how likely alternate bars are expected to form in a river reach*."

4.2. Definition of the Bar-Forming Discharge and the Associated Bar Height

When the criterion expressed by Equation 9 is satisfied, and then alternate bars are likely to form, a further question arises: what is the expected average bar height in the long-term?

To address this question, we propose the idea that the long-term average state of bars should correspond to the condition in which, accounting for the entire range of flow stages, the probabilities of growth and decay are balanced. In this perspective, we need to quantify the speed of bar height evolution, for the different flow stages.

In this case, the information that comes from the linear growth rate Ω_0 is no longer sufficient because the tendency of already-formed bars to grow or decay is significantly different from that displayed in the early stage of bar formation. This is clear when analyzing the behavior of bar height with time under steady flow conditions, resulting from the weakly nonlinear theory of Colombini et al. (1987) (see Figure 7). When the amplitude is relatively small, bars grow according to the linear growth rate Ω_0. However, as the amplitude increases, the bar growth gradually slows down, until the amplitude attains an equilibrium state. Furthermore, if the amplitude exceeds the equilibrium value, bars tend to decay, even under bar-forming conditions (i.e., $Q < Q_{cr}$).

In general, bar evolution can be quantified by means of the growth rate Ω (see Figure 7), whose absolute value specifies the rate of change of the bar amplitude, while its sign indicates whether bars tend to grow ($\Omega > 0$) or decay ($\Omega < 0$). Theoretical works suggest that the time evolution of the bar amplitude, for a given discharge value, follows a Landau-Stuart equation, in which the linear growth rate is multiplied by a correction term that depends on the square of the amplitude, namely:

$$\Omega := \frac{1}{A}\frac{dA}{dt} = \Omega_0\left[1 - kA^2\right], \tag{11}$$

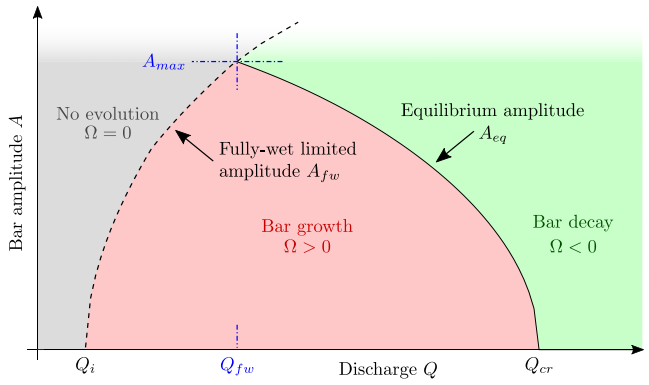

Figure 8. Morphological trajectory of alternate bars (defined by the sign of the growth rate Ω) depending on discharge and bar amplitude. Different regions (shaded areas) are delimited by the equilibrium amplitude (solid line) and the fully wet limited amplitude (dashed line), depending on discharge being higher or lower than the fully wet threshold Q_{fw} (see Redolfi et al., 2020). The point where the two lines intersect identifies the maximum bar amplitude A_{max}.

where the coefficient k is a function of discharge that can be estimated by means of nonlinear analyses (Bertagni & Camporeale, 2018; Colombini et al., 1987).

The bar topography resulting from nonlinear theories can be represented as the superimposition of harmonic components in longitudinal and transverse directions (see Colombini et al., 1987), from which the different metrics adopted to quantify bar height are readily derived, such as the elevation difference within a bar unit, H_{BM}, or the maximum value of the elevation differences calculated along individual cross-sections, H_B (see also Redolfi et al., 2020). The function A appearing in Equation 11 represents the amplitude of the dominant, first order, component of bed topography.

When $\Omega_0 > 0$ (i.e., under bar-forming conditions) the coefficient k is positive, and can be determined by the equilibrium condition $\Omega = 0$, which gives:

$$k = A_{eq}^{-2}, \tag{12}$$

so that Equation 11 can be expressed as:

$$\Omega(Q,A) := \frac{1}{A}\frac{dA}{dt} = \Omega_0\left[1 - \left(\frac{A}{A_{eq}}\right)^2\right]. \tag{13}$$

The term in square brackets in Equation 13 simply depends on the ratio between the current bar state and the equilibrium condition, and is always smaller than 1, possibly becoming negative when $A > A_{\mathrm{eq}}$.

Conversely, when $\Omega_0 < 0$ (i.e., under bar-suppressing conditions) the parameter k is negative. This implies that $\Omega < \Omega_0$, which means that finite-amplitude bars tend to decay more rapidly than small-amplitude bedforms.

The resulting scenario of evolutionary trajectories of bars, for the different values of flow discharge characterizing the hydrological cycle, is depicted in Figure 8. As highlighted in Section 2, the equilibrium amplitude A_{eq} vanishes at the critical threshold Q_{cr}. Hence, bar amplitude decays above such threshold and, for $Q < Q_{\mathrm{cr}}$, when its actual value is larger than A_{eq}. However, the asymptotic limit set by A_{eq} is not valid along the entire range of discharge states above the critical threshold Q_i. In fact, when the discharge is smaller than the so-called fully wet threshold Q_{fw} (see Adami et al., 2016) the theoretical estimate of the equilibrium amplitude is no longer meaningful, because the theory predicts bars whose top elevation, at equilibrium, would exceed the water surface level (which is not compatible with the fundamental model assumptions). To circumvent this limitation, we follow the approach suggested by Redolfi et al. (2020), assuming that within this range of discharges the bar growth is bounded by the fully wet value A_{fw}, which corresponds to the theoretical estimate of the amplitude when bars are at the onset of emerging from the water surface. Therefore, when $Q < Q_{\mathrm{fw}}$, the growth rate follows the same trend described by Equation 13, but with A_{fw} representing the asymptotic limit. The fully wet amplitude A_{fw} increases with the water discharge as illustrated in Figure 8 and sets the left margin of the region of bar growth. Beyond this limit, as for values of $Q < Q_i$, we assume a vanishing growth rate, which implies that low flow stages are unable to substantially rework already-formed bars whose crests emerge from the water surface.

In summary, depending on the actual values of bar amplitude and discharge, three distinct regions can be identified, as illustrated in Figure 8: (a) no evolution region, where the growth rate vanishes; (b) bar growth region, where Ω is positive; (c) bar decay region, where Ω is negative.

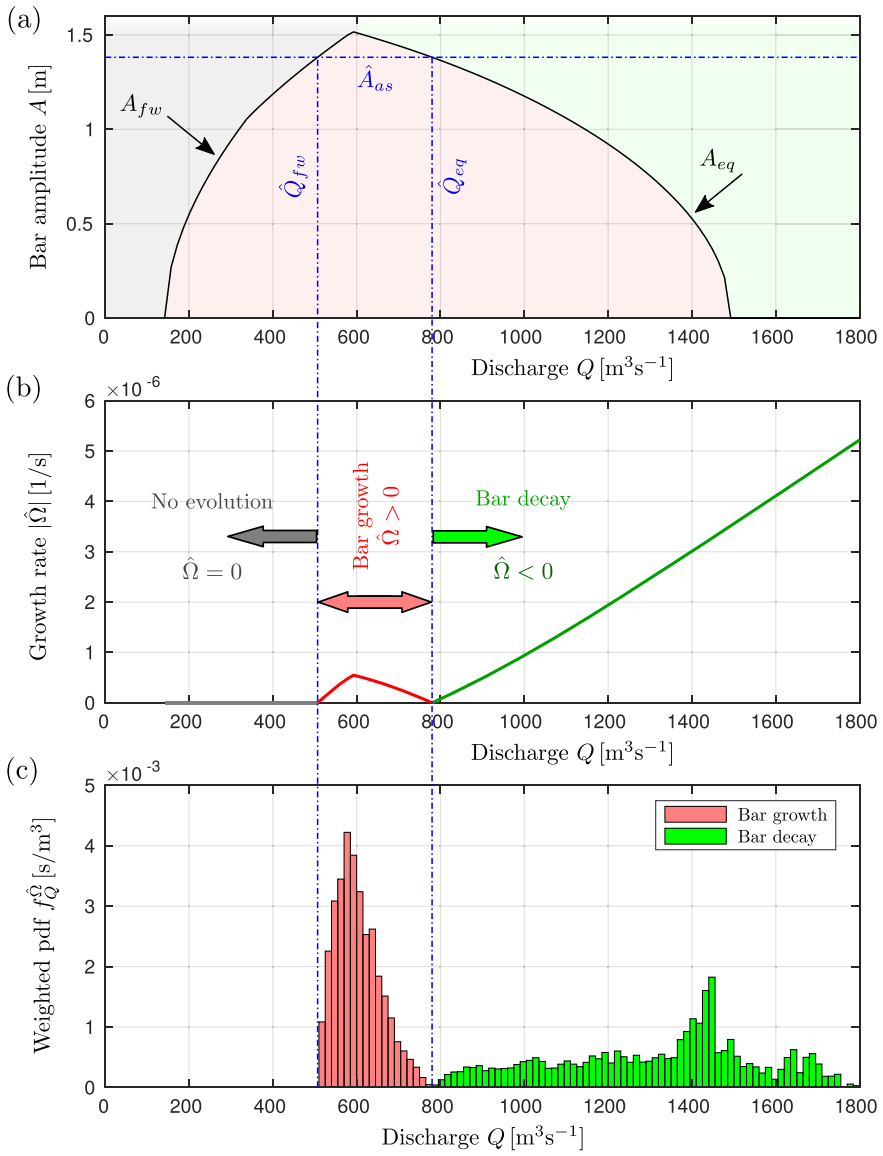

Figure 9. Illustration of the procedure for the evaluation of the average bar state: example of the upper reach of the Alpine Rhine River. (a) The regions of growth and decay, for a given value of the average bar amplitude $\hat{A}_{as}$. (b) The corresponding values of the growth rate $\hat{\Omega}$ for bars of amplitude $\hat{A}_{as}$. (c) Frequency of the flow events, weighted with the growth rate $\hat{\Omega}$, which measures the effectiveness of the different flow states. Bars are assumed to be in long-term equilibrium when the probability of bar growth (i.e., red area) equals the probability of bar decay (i.e., green area).

The above findings set the conceptual framework to define the average state of bars within a given river reach. With reference to Figure 9a, let us assume a tentative value of the average bar amplitude, $\hat{A}_{as}$, and compute the corresponding growth rate of bars for the different flow stages:

$$\hat{\Omega} := \Omega(Q, \hat{A}_{as}). \tag{14}$$

Moving from low to high flows at a fixed value of bar amplitude we cross the three regions highlighted in Figure 9a, which reflects on the resulting curve represented in Figure 9b. Specifically, if we denote by $\hat{Q}_{fw}$ and $\hat{Q}_{eq}$ the discharge values corresponding to the intersections with the fully wet threshold, A_{fw}, and the equilibrium amplitude, A_{eq} (see Figure 9a), the growth rate is positive when $\hat{Q}_{fw} < Q < \hat{Q}_{eq}$, otherwise it is either negative or vanishing.

We then define, as before, the scaled probability:

$$f_Q^{\hat{\Omega}} = \frac{f_Q\left|\hat{\Omega}\right|}{\int_0^\infty f_Q\left|\hat{\Omega}\right| dQ}, \tag{15}$$

which represents the effectiveness of the different discharge states in producing bar growth or decay, depending on the sign of $\hat{\Omega}$. The cumulative effectiveness of the events with positive $\hat{\Omega}$ (i.e., the red area of Figure 9c),

$$P_{growth}(\hat{A}_{as}) = \hat{P}(\hat{Q}_{fw} < Q < \hat{Q}_{eq}) = \int_{\hat{Q}_{fw}}^{\hat{Q}_{eq}} f_Q^{\hat{\Omega}} dQ, \tag{16}$$

defines the probability of bars with the given amplitude $\hat{A}_{as}$ to grow, while its complement, $(1 - P_{\text{growth}})$, measures the tendency to decay.

If $P_{\text{growth}} > 0.5$, bars of amplitude $\hat{A}_{as}$ are likely to experience a long-term growth, while the opposite tendency is expected when $P_{\text{growth}} < 0.5$. Therefore, we can assume that a long-term equilibrium is attained when:

$$P_{growth} = 0.5. \tag{17}$$

This condition implicitly defines the value of the long-term average bar amplitude A_{as}. In practice, this value can be obtained by varying $\hat{A}_{as}$ until the condition of Equation 17 is met, that is, when the red and the green areas of Figure 9a become equal.

Once the long-term average bar amplitude has been determined, we then compute the average-state bar topography and the associated bar height, through the weakly nonlinear solution of Colombini et al. (1987), and we define a bar-forming discharge, Q_{form}, as the value of discharge $\hat{Q}_{eq}$ associated with the resulting average bar amplitude. Therefore, Q_{form} is the discharge that if maintained indefinitely would produce the same long-term bar topography as the river hydrograph.

5. Results

We now apply the methodology developed in Section 4 to the four study cases described in Section 3: A summary of model results is reported in Table 2. The procedure is based on two steps:

1. We first provide a criterion for evaluating whether bars are likely to form, which is based on the idea that this depends on how long the river stays in bar-forming conditions with respect to bar-suppressing conditions. The key novelty is that the duration of different flow stages is measured in the time of the bars, rather than in absolute time. This is accomplished by multiplying the flow probability density function by the linear bar growth rate, and comparing the weight of the resulting distributions that falls above or below the critical threshold for bar formation, Q_{cr}.
2. We then provide a criterion for estimating the long-term bar topography, which is based on the idea that the average state of bars corresponds to conditions for which the probabilities of bar growth and decay are equal. The key ingredient is that the effectiveness of the different discharge states not only depends on the discharge value, but also on bar amplitude, as suggested by nonlinear bar theories. Specifically, the higher is the bar, the wider is the range of discharge states for which bar amplitude tends to decay.

5.1. The Case of the Alpine Rhine River

In the case of the upstream reach of the Alpine Rhine River, the value of probability resulting from Equation 8 is very high ($P_{\text{form}} = 0.99$, see Table 2), which indicates that alternate bars are very likely to form. Conversely, in the downstream reach the probability is around 50% ($P_{\text{form}} = 0.58$), which reveals that the total work of bar-forming and bar-suppressing events (red and green area of Figure 6b) almost balances.

Table 2
Summary of Model Results for the Four Study Cases, as Obtained With the Transport Formulas of Parker (1978) (P78) and Meyer-Peter and Muller (1948) (MPM)

	Alpine Rhine							
	Upstream		Downstream		Isère		Adige	
	P78	MPM	P78	MPM	P78	MPM	P78	P78
Q_{eff} ($m^3 s^{-1}$)	405	435	465	465	330	350	1387	1388
$T_r(Q_{\text{eff}})$ (y)	1	1	1	1	1.19	1.26	16.37	16.43
Q_i ($m^3 s^{-1}$)	142	304	116	246	130	278	494	1048
Q_{cr} ($m^3 s^{-1}$)	1493	1278	467	456	1326	1136	938	1248
$T_r(Q_{\text{cr}})$ (y)	5.05	3.06	1	1	>200	>200	3.45	9.93
Q_{fw} ($m^3 s^{-1}$)	585	615	255	345	530	550	788	1213
$T_r(Q_{\text{fw}})$ (y)	1.06	1.08	1	1	2.87	3.23	2.19	8.77
P_{form} (%)	99.9	99.8	57.9	56.8	100.0	100.0	11.4	16.7
$\Omega_{0,\,\max}$ (d^{-1})	0.284	0.461	0.070	0.196	0.578	0.952	0.005	0.050
$\bar{H}_B$ (m)	2.4	2.5	0.49	0.53	2.6	2.7	0	0
Q_{form} ($m^3 s^{-1}$)	778	717	442	421	602	602	-	-
$T_r(Q_{\text{form}})$ (y)	1.25	1.17	1	1	4.45	4.45	-	-

Note. Q_{eff} is the effective discharge value resulting from the method of Wolman and Miller (1960), Q_i and Q_{cr} are the critical values for incipient sediment motion and for bar formation, respectively, Q_{fw} is the fully wet threshold, P_{form} is the probability of bar-forming events, $\Omega_{0,\,\max}$ is the maximum bar growth rate, $\bar{H}_B$ is the average bar height, Q_{form} is the corresponding bar-forming discharge, and T_r indicates the return period of the reported discharge values. When P_{form} is smaller than 50%, as in the case of the Adige River, bars are not expected to form.

Therefore, the average state is close to the limiting conditions for bar formation, in which bars that might possibly form would attain an almost vanishing amplitude.

We then compute the average-state bar topography and the associated bar height. Being based on extreme elevation values, the above-mentioned metrics H_{BM} and H_B are difficult to derive from field data, as different sources of measurement uncertainty exist and available cross-sectional data do not necessarily comprise the points of maximum and minimum elevation. Therefore, for comparison with field data we compute the mean value of the cross-sectional elevation differences in a bar wavelength, $\bar{H}_B$. Results illustrated in Table 2 reveal that the estimated long-term bar height $\bar{H}_B$ in the upstream reach of the Alpine Rhine River is about 2.5 m for both the tested sediment transport relations, while a much smaller value ($\bar{H}_B \simeq 0.5$ m) is obtained for the downstream reach. This is in overall agreement with field measurements based on cross-sectional elevation data. Specifically, data for the upstream reach reported in Adami et al. (2016) (see their Figure 9) display cross-sectional elevation differences in the range from 2.5 to 4.0 m, while for the downstream reach we observe low-relief, submerged bars with an average height of about 0.4 m. This comparison highlights the potential of our methodology to evaluate the long-term bar topography, though the theory slightly underestimates the observed bar height in the upstream reach. However, this difference can be easily corrected by tuning the empirical coefficient r that measures the effect of the lateral bed slope on bed-load transport. It is worth noticing that the proposed procedure provides a sound interpretation of the different bed response exhibited by two consecutive reaches of the Alpine Rhine River, upstream and downstream the confluence of the Ill River.

As reported in Table 2, the resulting values of the bar-forming discharge, Q_{form}, for the upstream reach of the Rhine River range from 720 to 780 $m^3 s^{-1}$, depending on the transport formula used, and the associated return period is only slightly longer than one year. For the downstream reach, the discharge value is very close to the critical threshold, which confirms the river's weak propensity to form alternate bars. We note that the value of the bar-forming discharge is larger than that of effective discharge Q_{eff} in the upstream reach, while the opposite occurs in the downstream reach.

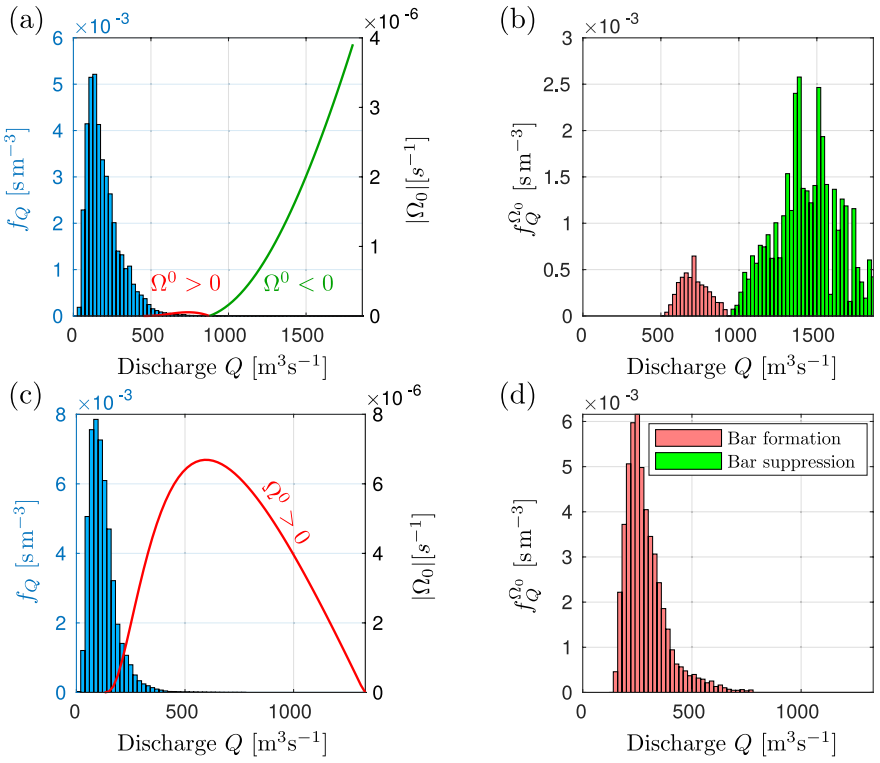

Figure 10. The scaled probability function for the Adige River (a, b) and for the Isère River (c, d), obtained by multiplying the flow probability density function f_Q (histograms on the left panels) by the absolute value of linear bar growth rate $|\Omega_0|$ (solid line). The resulting histograms on the right panels represents the effectiveness of different flow states to form (red area) and to suppress (green area) alternate bars.

Results reported in Table 2 show that the proposed criterion for bar occurrence, which is based on P_{form}, and the predicted values of the average bar height and bar-forming discharge are almost independent of the adopted sediment transport formula. They also suggest that the different behavior displayed by the downstream reach is mainly a consequence of the reduction of the critical bar threshold, and of the corresponding return period, due to its smaller channel width. Therefore, while bar-suppressing stages are extremely rare in the upstream reach, they become much more frequent in the downstream reach, which results in a barely visible bar pattern. Furthermore, the maximum positive value of the growth rate $\Omega_{0,\,\max}$ (see Table 2) is larger for the upstream reach. We note that $\Omega_{0,\,\max}$ provides an estimate of the timescale required for bar evolution, which is of the order of a few days for the upstream reach of the Rhine River. Such estimate, when combined with the resulting value of the return period of the bar forming discharge Q_{form}, suggests that bar topography in the upper Rhine may undergo significant changes during yearly recurring flood events.

5.2. The Cases of the Adige and the Isère River

The study reach of the Adige River is characterized by an almost flat bed morphology and therefore represents a sort of limit case of the downstream Rhine River reach. Bar-suppressing events dominate over the bar-forming counterparts, as illustrated in Figure 10b. Therefore, the resulting probability P_{form} is well below 0.5, as reported in Table 2, which implies that the formation of bars is very unlikely. We note that the presence of an armored bed surface, with a relatively large sediment size, produces a twofold effect: (a) the threshold for sediment motion Q_i is quite large and gets closer to the critical value Q_{cr}, which makes the flow events able to mobilize the riverbed relatively rare, while narrowing the range of bar-forming events; (b) the maximum positive value of the growth rate $\Omega_{0,\,\max}$ (see Table 2) is quite small, say one-two orders of magnitude smaller than for the Rhine River, meaning that the process of bar formation is very slow. This implies that bar-forming events in the Adige River are not only less effective than bar-suppressing events,

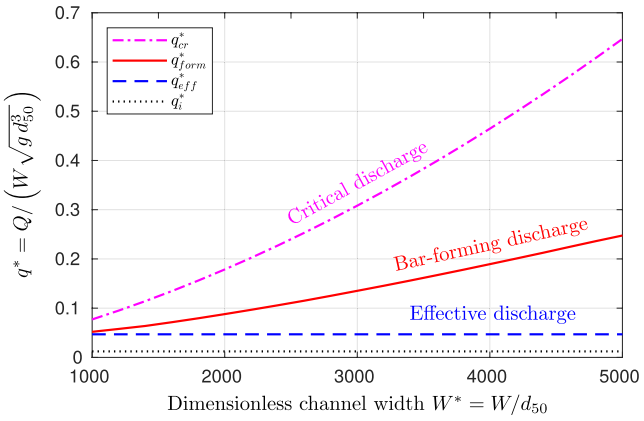

Figure 11. Variation of unitary (i.e., per unit width) dimensionless values of: (i) effective (dashed line), (ii) bar-forming (solid line), (iii) critical (dash-dot line), and (iv) incipient-motion (dotted line) discharges with the dimensionless channel width, considering an ideal experiment where the mean unitary discharge is kept constant. The diverging trend of the associated curves highlights the remarkably different response of the bar-forming discharge and the effective discharge to variations of river parameters. All quantities are made dimensionless as suggested by Parker et al. (2007). Example with channel slope $S = 0.30\%$, coefficient of variation $c_v = 0.7$ and mean dimensionless discharge per unit width $\overline{q}^* = \overline{Q} / (W\sqrt{g d_{50}^3}) = 80$.

but they are also characterized by a very low effectiveness in absolute terms. A flood event lasting tens/hundreds of days within the formative range ($Q_i < Q < Q_{cr}$) would be required to allow a significant bar growth.

The case of the Isère River represents an opposite situation with respect to the Adige River, as the study reach displays a stable sequence of high-relief vegetated bars, whose average height $\overline{H}_B$ is about 3.5 m. The river width is such that the threshold value Q_{cr} is very high, the return period being above 200 years, and therefore bar-suppressing events are extremely unlikely. The scaled probability function reported in Figure 10d closely resembles that of the upper Rhine River. However, the return period of both the resulting bar-forming discharge Q_{form}, which is about 600 $m^3\ s^{-1}$, and of the fully wet threshold Q_{fw} is much longer. This implies that flood events able to substantially rework the bar topography are relatively rare in the Isère River, which provides a favorable condition for vegetation development. The above findings are confirmed by the results of the numerical investigations of Jourdain et al. (2020), who analyzed the influence of large events on bar dynamics in the Isère River, accounting for the role of riparian vegetation, and found that the actual equilibrium morphology of bars and vegetation cover can be associated with large floods, with a peak value on the order of 800 $m^3\ s^{-1}$. We also note that the predicted average bar height $\overline{H}_B$ resulting from our procedure, about 2.7 m, is in reasonable agreement with field measurements.

6. Discussion

6.1. Effective and Bar-Forming Discharge

The novel concept of bar-forming discharge proposed in this work significantly differs from the classical definition of effective discharge also in terms of its dependence on river characteristics. To highlight this difference, we analyze the effect of changing the channel width on the computed values of Q_{form} and Q_{eff}.

We take a two-parameter distribution to describe the probability density function of flow events, such that it can be specified by fixing the mean discharge $\overline{Q}$ and the coefficient of variation c_v. Specifically, we consider a log-normal distribution (Bowers et al., 2012; Castellarin et al., 2004), which has been proven to effectively reproduce the flow frequency distribution in the Rhine River (see Bertagni et al., 2018). We then imagine an ideal experiment where the channel width is varied, while maintaining constant values of the mean unitary discharge, $\overline{q} = \overline{Q} / W$, slope, grain size and coefficient of variation, and compute the effective and bar-forming discharges, as well as the key threshold values Q_i and Q_{cr}.

The resulting values, set in terms of unitary (i.e., per unit width) discharges and made dimensionless according to Parker et al. (2007), are illustrated in Figure 11. It appears that the bar-forming unitary discharge exhibits an explicit dependence on channel width, while the effective discharge remains constant. Such different behavior is a consequence of the variations with the channel width of the key threshold values: the unitary discharge value corresponding to the incipient sediment motion keeps constant, while the critical discharge for bar formation increases as the channel gets wider. We note that an analogous behavior is obtained when changing the channel slope.

This analysis highlights the sensitivity of the bar-forming discharge to river parameters, and marks a clear difference with respect to the effective discharge, whose dependence on river characteristics merely results from changes of the Shields parameter.

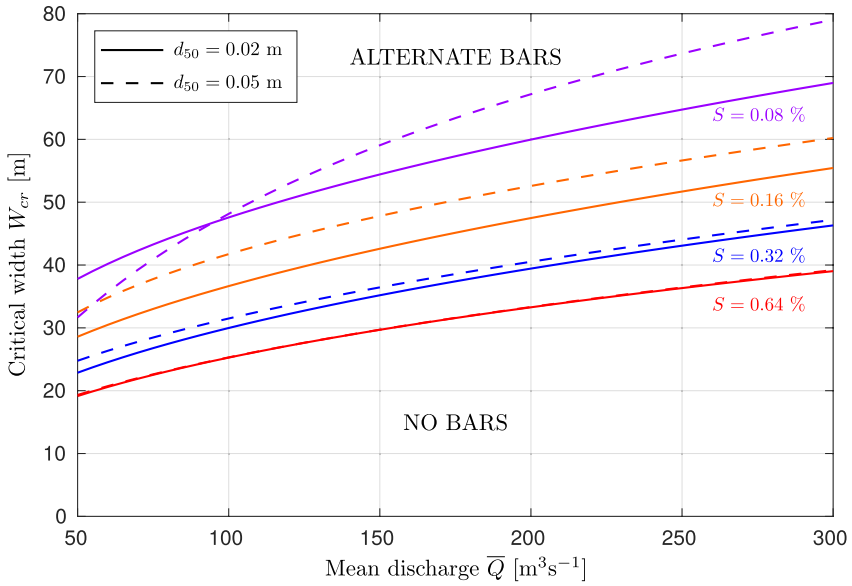

Figure 12. Critical channel width as a function of the mean discharge, for different values of channel slope (S) and median grain size (d_{50}), with dashed lines indicating the coarser bed material. Alternate bars are expected to form when the channel width exceeds the critical threshold W_{cr}. Example with fixed coefficient of variation $c_v = 0.7$.

6.2. A Criterion for Bar Formation Under Unsteady Flow Conditions

The criterion for bar formation defined by Equation 9 can be generalized by plotting marginal curves that identify the regions of bar occurrence in the space of the key controlling parameters. In particular, for given values of flow and river parameters it is possible to identify a threshold channel width, W_{cr}, which discriminates channels where alternate bars are likely to develop from cases where no bars are expected. This enables for building bar existence diagrams, such as that illustrated in Figure 12, where values of parameters typical of gravel bed rivers have been considered.

The critical width increases with the mean discharge, for given values of slope and grain size. This is because at higher flow values the mean duration of bar-suppressing events expands, so that wider channels are needed to allow for bar formation. The role of channel slope and grain size variations is more subtle, as it depends on the associated changes of the threshold discharge values, Q_i and Q_{cr}, that define, for given $\overline{Q}$, the lower and upper limits of the range of bar-forming stages.

On one hand, increasing the channel slope lowers the threshold for incipient sediment motion Q_i, and therefore the region of bar occurrence widens, the more so because the critical threshold Q_{cr} generally increases with the channel slope. As a result, the critical width W_{cr} gets smaller. However, at relatively low values of the Shields parameter θ the critical discharge displays an opposite, decreasing trend with the channel slope, which reflects the sharp increase with θ of the critical width-to-depth ratio β_{cr} predicted by bar theories (see Figure 6 of Colombini et al., 1987). This implies that the effect of slope on W_{cr} becomes weaker (and possibly reverses). We note that, in terms of the parameters employed in Figure 12, the Shields parameter gets smaller when both the mean discharge and the channel slope are relatively low and the sediment is coarser (dashed lines of Figure 12). On the other hand, increasing the grain size leads to contrasting effects on bar formation because Q_i gets larger and also Q_{cr} generally increases (see again Figure 6 of Colombini et al., 1987). The net effect of the competition between these two factors leads to an overall increase of the critical width as the sediment gets coarser, except for relatively low values of mean discharge and channel slope. Moreover, the effect of grain size reduces when raising the channel slope, becoming practically irrelevant for $S > 0.5\%$.

6.3. Limitations and Future Perspectives

The procedure outlined in Section 4 to define the long-term bar height, and the corresponding formative discharge, is based on the assumption that the bar state can be represented by the average amplitude A_{as}, so that the long term bar evolution merely depends on the expected frequency of the different discharge states. Specifically, Equation 14 accounts for the effect of discharge changes on the growth rate, while it neglects the role of bar amplitude variations with respect to the average state, which may occur during individual flow events. These fluctuations can produce a net effect on the average growth rate, and therefore on the average bar height. However, as demonstrated by Carlin et al. (2020), their role is usually negligible when bar adaptation to changing discharge is comparatively slow (see Tubino, 1991), to such an extent that individual flow events are not capable to produce strong modifications of bar height. Conversely, the dependence of bar growth on the instantaneous bar amplitude becomes relevant when the characteristic duration of flood events is long enough to heavily rework bar topography. In this case, one should resort to different metrics to fully characterize, in a statistical sense, the flow regime, because the definition of the average state of bars would require to take into account the duration and sequencing of the individual flow events, an information that is not contained in the flow probability density function.

In our analysis we have assumed that the alternate mode, $m = 1$, is the dominant transverse mode of bar topography, as it is often the case of channelized river reaches. However, higher order modes (e.g., central bars) can also develop in relatively wide channels, specifically at low flow stages (i.e., at large width-to depth ratio values), provided their respective critical discharge exceeds the threshold for incipient sediment motion. The proposed methodology can be readily extended to determine the conditions for the possible formation of higher modes. For example, to assess whether central (i.e., $m = 2$) bars may form, we can compute their linear growth rate $\Omega_0\,(m = 2)$ and repeat the same procedure outlined in Section 4 to obtain the associated probability $P_{\text{form}}\,(m = 2)$. We note, however, that in this case the condition expressed by Equation 9 is no longer sufficient because both the alternate and central bar modes are simultaneously unstable, and therefore an additional criterion is required to determine the dominant mode resulting from their competition. Ultimately, a fully nonlinear, numerical solution would be required to determine the outcome of such competition. However, a common, albeit approximate criterion is based on selecting the mode that displays the higher linear growth rate for a given discharge (e.g., Fredsoe, 1978; Seminara & Tubino, 1989). A straightforward way to extend this criterion to the entire river hydrograph is to compute the mean growth rate, defined as in Equation 10, and to compare the resulting values for the two modes. Two out of the four study cases analyzed in Section 5 return a value of $P_{\text{form}}\,(m = 2)$ higher than 0.5, namely (and not surprisingly) the upstream reach of the Alpine Rhine River and the Isère River, suggesting that central bars might potentially form, especially at low flow stages. However, in both cases we obtain $\overline{\Omega}_0(m = 1) > \overline{\Omega}_0(m = 2)$, which implies that the alternate bar mode dominates. A detailed validation of this procedure is beyond the scope of the present work, as it would require the analysis of more comprehensive data set, along with a comparison with alternative criteria based on the amplification of non-migrating bars (e.g., Crosato & Mosselman, 2009).

Finally, it is worth highlighting that in this study we focus on gravel bed rivers, or at least on cases where most of the sediment is transported as bedload. However, our methodology can be naturally extended to rivers dominated by suspended sediment transport, provided that growth rate and equilibrium amplitude are suitably computed (e.g., by means of the weakly nonlinear theory of Bertagni & Camporeale, 2018). In this case, even more attention is probably needed to investigate the competition among different unstable modes (Tubino et al., 1999) and the possible interaction between bars and migrating dunes (Colombini & Stocchino, 2012).

7. Conclusions

In this work, we have investigated the response of bar topography to the hydrological regime in channelized river reaches, coupling the information derived from the statistical distribution of flow events with the theoretical predictions obtained from the weakly nonlinear model of Colombini et al. (1987). The recognition that the long-term bar topography results from the combined effect of bar-forming ordinary floods and of bar-suppressing large events ultimately represents the key novelty of this work. On the basis of the results of our study and the analysis of four gravel bed river reaches, we can draw the following conclusions:

1. We propose a novel criterion for determining whether free alternate bars are expected to form in a river reach, which depends on channel characteristics and on the probability distribution of flow events. The criterion is not merely based on the time spent by the river in bar-forming and bar-suppressing conditions, but also considers the effectiveness of the different discharge states, as measured by the linear bar growth rate.
2. The above criterion entails the definition of a threshold channel width W_{cr} that sets the transition between two different morphological styles. Modeling the response of bar topography by means of a theoretical model allows for analyzing the dependence of the threshold width on the key physical parameters.
3. When the river width is larger than W_{cr}, we propose a procedure for estimating the average bar height, which results from a long-term balance between the enhancing effect of moderate flow events and the opposite effect of more intense flood events.
4. The long-term average bar state allows us to define a bar-forming discharge as the value that, if applied steadily, would give the same bar amplitude as the hydrological regime. Differently from the effective discharge (Wolman & Miller, 1960), the bar-forming discharge is highly sensitive to variations of river characteristics, primarily the channel width.

The proposed method provides a sound interpretation of the markedly distinct bed configuration displayed by different gravel bed river reaches, along with a reasonable estimate of the long-term bar height resulting from a complex sequence of flow events. Therefore, the procedure could be suited to various applications, such as the analysis of long-term morphological trajectories following different scenarios of hydrological alterations (e.g., climate change, hydropower exploitation) and river engineering interventions (e.g., channel widening).

Data Availability Statement

The MATLAB code for computing probability of bar formation, average bar height and bar-forming discharge depending on channel geometry, grain size and flow probability distribution, as well as data of the four study reaches, are made available at https://doi.org/10.5281/zenodo.4277627.

Acknowledgments
This research has been supported by the Italian Ministry of Education, University and Research (MIUR) in the framework of the "Departments of Excellence" (grant no. L. 232/2016). The study has benefited from the insightful comments by Alessandra Crosato and two anonymous referees.

References

Adami, L., Bertoldi, W., & Zolezzi, G. (2016). Multidecadal dynamics of alternate bars in the Alpine Rhine River. *Water Resources Research*, *52*, 8938–8955. https://doi.org/10.1002/2015WR018228

Andrews, E. D. (1980). Effective and bankfull discharges of streams in the Yampa River basin, Colorado and Wyoming. *Journal of Hydrology*, *46*, 311–330. https://doi.org/10.1016/0022-1694(80)90084-0

Ashmore, P. E., & Day, T. J. (1988). Effective discharge for suspended sediment transport in streams of the Saskatchewan River Basin. *Water Resources Research*, *24*(6), 864–870. https://doi.org/10.1029/WR024i006p00864

Baker, V. R. (1977). Stream-channel response to floods, with examples from central Texas. *Bulletin of the Geological Society of America*, *88*(8), 1057–1071. https://doi.org/10.1130/0016-7606(1977)88<1057:srtfwe>2.0.co;2

Barry, J. J., Buffington, J. M., Goodwin, P., Asce, M., King, J. G., & Emmett, W. W. (2008). Performance of bed-load transport equations relative to geomorphic significance: Predicting effective discharge and its transport rate. *Journal of Hydraulic Engineering*, *134*(5), 601–615. https://doi.org/10.1061/(ASCE)0733-942910.1061/(asce)0733-9429(2008)134:5(601)

Benson, M. A., & Thomas, D. M. (1966). A definition of dominant discharge. *International Association of Scientific Hydrology Bulletin*, *11*(2), 76–80. https://doi.org/10.1080/02626666609493460

Bertagni, M. B., & Camporeale, C. (2018). Finite amplitude of free alternate bars with suspended load. *Water Resources Research*, *54*(12), 9759–9773. https://doi.org/10.1029/2018WR022819

Bertagni, M. B., Perona, P., & Camporeale, C. (2018). Parametric transitions between bare and vegetated states in water-driven patterns. *Proceedings of the National Academy of Sciences*, *115*(32), 8125–8130. https://doi.org/10.1073/pnas.1721765115

Biedenharn, D. S., & Thorne, C. R. (1994). Magnitude-frequency analysis of sediment transport in the lower Mississippi river. *Regulated Rivers: Research & Management*, *9*(4), 237–251. https://doi.org/10.1002/rrr.3450090405

Blom, A., Arkesteijn, L., Chavarrías, V., & Viparelli, E. (2017). The equilibrium alluvial river under variable flow and its channel-forming discharge. *Journal of Geophysical Research: Earth Surface*, *122*(10), 1924–1948. https://doi.org/10.1002/2017JF004213

Bowers, M. C., Tung, W. W., & Gao, J. B. (2012). On the distributions of seasonal river flows: Lognormal or power law? *Water Resources Research*, *48*(5), W05536. https://doi.org/10.1029/2011WR011308

Carlin, M., Redolfi, M., & Tubino, M. (2020). *Effect of flow unsteadiness on the long term evolution of alternate bars*. Proceedings of river flow (pp. 539–547). CRC Press. https://doi.org/10.1201/b22619-76

Carling, P. (1988). The concept of dominant discharge applied to two gravel-bed streams in relation to channel stability thresholds. *Earth Surface Processes and Landforms*, *13*(4), 355–367. https://doi.org/10.1002/esp.3290130407

Castellarin, A., Galeati, G., Brandimarte, L., Montanari, A., & Brath, A. (2004). Regional flow-duration curves: Reliability for ungauged basins. *Advances in Water Resources*, *27*, 953–965. https://doi.org/10.1016/j.advwatres.2004.08.005

Church, M., & Ferguson, R. I. (2015). Morphodynamics: Rivers beyond steady state. *Water Resources Research*, *51*(4), 1883–1897. https://doi.org/10.1002/2014WR016862

Colombini, M., Seminara, G., & Tubino, M. (1987). Finite-amplitude alternate bars. *Journal of Fluid Mechanics*, *181*, 213–232. https://doi.org/10.1017/S0022112087002064

Colombini, M., & Stocchino, A. (2012). Three-dimensional river bed forms. *Journal of Fluid Mechanics*, *695*, 63–80. https://doi.org/10.1017/jfm.2011.556

Crosato, A., Desta, F. B., Cornelisse, J., Schuurman, F., & Uijttewaal, W. S. J. (2012). Experimental and numerical findings on the long-term evolution of migrating alternate bars in alluvial channels. *Water Resources Research*, *48*(6), W06524. https://doi.org/10.1029/2011WR011320

Crosato, A., & Mosselman, E. (2009). Simple physics-based predictor for the number of river bars and the transition between meandering and braiding. *Water Resources Research*, *45*(3), W03423. https://doi.org/10.1029/2008WR007242

Crosato, A., Mosselman, E., Desta, F. B., & Uijttewaal, W. S. J. (2011). Experimental and numerical evidence for intrinsic nonmigrating bars in alluvial channels. *Water Resources Research*, *47*(3), W03511. https://doi.org/10.1029/2010WR009714

Crowder, D. W., & Knapp, H. V. (2005). Effective discharge recurrence intervals of Illinois streams. *Geomorphology*, *64*(3–4), 167–184. https://doi.org/10.1016/j.geomorph.2004.06.006

Defina, A. (2003). Numerical experiments on bar growth. *Water Resources Research*, *39*(4), 1092. https://doi.org/10.1029/2002WR001455

Diaz-Redondo, M., Egger, G., Marchamalo, M., Hohensinner, S., & Dister, E. (2017). Benchmarking fluvial dynamics for process-based river restoration: The upper Rhine river (1816-2014). *River Research and Applications*, *33*, 403–414. https://doi.org/10.1002/rra.3077

Downs, P. W., Soar, P. J., & Taylor, A. (2016). The anatomy of effective discharge: The dynamics of coarse sediment transport revealed using continuous bedload monitoring in a gravel-bed river during a very wet year. *Earth Surface Processes and Landforms*, *41*(2), 147–161. https://doi.org/10.1002/esp.3785

Doyle, M. W., Shields, D., Boyd, K. F., Skidmore, P. B., & Dominick, D. (2007). Channel-Forming Discharge Selection in River Restoration Design. *Journal of Hydraulic Engineering*, *133*(7), 831–837. https://doi.org/10.1061/(ASCE)0733-942910.1061/(asce)0733-9429(2007)133:7(831)

Dynesius, M., & Nilsson, C. (1994). Regulation of river systems in the northern third of the world. *Science*, *266*(5186), 753–762. https://doi.org/10.1126/science.266.5186.753

Eekhout, J. P., Hoitink, A. J., & Mosselman, E. (2013). Field experiment on alternate bar development in a straight sand-bed stream. *Water Resources Research*, *49*(12), 8357–8369. https://doi.org/10.1002/2013WR014259

Emmett, W. W., & Wolman, M. G. (2001). Effective discharge and gravel-bed rivers. *Earth Surface Processes and Landforms*, *26*(13), 1369–1380. https://doi.org/10.1002/esp.303

Engelund, F., & Fredsoe, J. (1982). Sediment ripples and dunes. *Annual Review of Fluid Mechanics*, *14*, 13–37. https://doi.org/10.1146/annurev.fl.14.010182.000305

Federici, B., & Seminara, G. (2006). Effect of suspended load on sandbar instability. *Water Resources Research*, *42*(7), W07407. https://doi.org/10.1029/2005WR004399

Ferro, V., & Porto, P. (2012). Identifying a dominant discharge for natural rivers in southern Italy. *Geomorphology*, 139–140, 313–321. https://doi.org/10.1016/j.geomorph.2011.10.035

Fredsoe, J. (1978). Meandering and braiding of rivers. *Journal of Fluid Mechanics*, *84*(4), 609–624. https://doi.org/10.1017/S0022112078000373

Goodwin, P. (2004). Analytical solutions for estimating effective discharge. *Journal of Hydraulic Engineering*, *130*(8), 729–738. https://doi.org/10.1061/(ASCE)0733-942910.1061/(asce)0733-9429(2004)130:8(729)

Hall, P. (2004). Alternating bar instabilities in unsteady channel flows over erodible beds. *Journal of Fluid Mechanics*, *499*, 49–73. https://doi.org/10.1017/S0022112003006219

Hohensinner, S., Egger, G., Haidvogl, G., Jungwirth, M., Muhar, S., & Schmutz, S. (2007). Hydrological connectivity of a Danube river-floodplain system in the Austrian Machland: Changes between 1812 and 1991. In S. A. S. Lavoisier (Ed.), *Proceedings of the international conference "European floodplains 2002"* (pp. 53–69). Strasbourg (France).

Ikeda, S. (1984). Prediction of alternate bar wavelength and height. *Journal of Hydraulic Engineering*, *110*(4), 371–386. https://doi.org/10.1061/(ASCE)0733-942910.1061/(asce)0733-9429(1984)110:4(371)

Inglis, C. C. (1949). *The behaviour and control of rivers and canals (with the aid of models)*. Poona, India: Yeravda Prison Press.

Jaballah, M., Camenen, B., Pénard, L., & Paquier, A. (2015). Alternate bar development in an alpine river following engineering works. *Advances in Water Resources*, *81*, 103–113. https://doi.org/10.1016/j.advwatres.2015.03.003

Jaeggi, M. N. R. (1984). Formation and effects of alternate bars. *Journal of Hydraulic Engineering*, *110*(2), 142–156. https://doi.org/10.1061/(ASCE)0733-942910.1061/(asce)0733-9429(1984)110:2(142)

Jäggi, M. (1983). *Alternierende Kiesbanke (Alternate bars)*. Swiss Federal Institute of Technology Zürich Laboratory of Hydraulics, Hydrology and Glaciology, Switzerland.

Jourdain, C., Claude, N., Tassi, P., Cordier, F., & Antoine, G. (2020). Morphodynamics of alternate bars in the presence of riparian vegetation. *Earth Surface Processes and Landforms*, *45*(5), 1100–1122. https://doi.org/10.1002/esp.4776

Kinoshita, R. (1961). *Investigation of channel deformation in Ishikari river* (p. 174). Japan: Report of Bureau of Resourcess, Department of Science and Technology.

Lanzoni, S. (2000). Experiments on bar formation in a straight flume: 1. Uniform sediment. *Water Resources Research*, *36*(11), 3337–3349. https://doi.org/10.1029/2000WR900160

Leopold, L. B., & Wolman, G. M. (1957). *River channel patterns: Braided, meandering, and straight*. US Government Printing Office.

Mähr, M., Schenk, D., Schatzmann, M., & Meng, A. (2014). Alpine rhine project (section river Ill-lake constance). *Proceedings of the international conference on fluvial hydraulics, river flow* (pp. 39–47). https://doi.org/10.1201/b17134-7

Meyer-Peter, E., & Muller, R. (1948). Formulas for bed-load transport. *IAHSR 2nd meeting*. Stockholm: IAHR.

Molle, F. (2009). River-basin planning and management: The social life of a concept. *Geoforum*, *40*(3), 484–494. https://doi.org/10.1016/j.geoforum.2009.03.004

Nash, D. B. (1994). Effective sediment-transporting discharge from magnitude-frequency analysis. *The Journal of Geology*, *102*(1), 79–95. https://doi.org/10.1086/629649

Nelson, J. M. (1990). The initial instability and finite-amplitude stability of alternate bars in straight channels. *Earth Science Reviews*, *29*(1–4), 97–115. https://doi.org/10.1016/0012-8252(0)90030-Y

Nelson, P. A., & Morgan, J. A. (2018). Flume experiments on flow and sediment supply controls on gravel bedform dynamics. *Geomorphology*, *323*, 98–105. https://doi.org/10.1016/j.geomorph.2018.09.011

Nilsson, C., Reidy, C. A., Dynesius, M., & Revenga, C. (2005). Fragmentation and flow regulation of the world's large river systems. *Science*, *308*(5720), 405–408. https://doi.org/10.1126/science.1107887

Parker, G. (1976). On the cause and characteristic scales of meandering and braiding in rivers. *Journal of Fluid Mechanics*, *76*(3), 457–480. https://doi.org/10.1017/S0022112076000748

Parker, G. (1978). Self-formed rivers with equilibrium banks and mobile bed. Part 2. The gravel river. *Journal of Fluid Mechanics*, *89*(1), 127–146. https://doi.org/10.1017/S0022112078002505

Parker, G., Wilcock, P. R., Paola, C., Dietrich, W. E., & Pitlick, J. (2007). Physical basis for quasi-universal relations describing bankfull hydraulic geometry of single-thread gravel bed rivers. *Journal of Geophysical Research: Earth Surface*, *112*(F4), F04005. https://doi.org/10.1029/2006JF000549

Pickup, G., & Warner, R. F. (1976). Effects of hydrologic regime on magnitude and frequency of dominant discharge. *Journal of Hydrology*, *29*(1–2), 51–75. https://doi.org/10.1016/0022-1694(76)90005-6

Qian, H., Cao, Z., Liu, H., & Pender, G. (2017). Numerical modelling of alternate bar formation, development and sediment sorting in straight channels. *Earth Surface Processes and Landforms*, *42*(4), 555–574. https://doi.org/10.1002/esp.3988

Redolfi, M., Welber, M., Carlin, M., Tubino, M., & Bertoldi, W. (2020). Morphometric properties of alternate bars and water discharge: A laboratory investigation. *Earth Surface Dynamics*, *8*(3), 789–808. https://doi.org/10.5194/esurf-8-789-2020

Rodrigues, S., Mosselman, E., Claude, N., Wintenberger, C. L., & Juge, P. (2015). Alternate bars in a sandy gravel bed river: Generation, migration and interactions with superimposed dunes. *Earth Surface Processes and Landforms*, *40*(5), 610–628. https://doi.org/10.1002/esp.3657

Scorpio, V., Zen, S., Bertoldi, W., Surian, N., Mastronunzio, M., Dai Prá, E., et al. (2018). Channelization of a large Alpine river: What is left of its original morphodynamics? *Earth Surface Processes and Landforms*, *43*(5), 1044–1062. https://doi.org/10.1002/esp.4303

Selby, M. J. (1974). Dominant geomorphic events in landform evolution. *Bulletin of the International Association of Engineering Geology*, *9*, 85–89. https://doi.org/10.1007/BF02635309

Seminara, G., & Tubino, M. (1989). Alternate bars and meandering: Free, forced and mixed interactions. In S. Ikeda, & G. Parker (Eds.), *River meandering* (pp. 267–320). Washington, DC: American Geophysical Union (AGU). https://doi.org/10.1029/WM012p0267

Serlet, A. J., Gurnell, A. M., Zolezzi, G., Wharton, G., Belleudy, P., & Jourdain, C. (2018). Biomorphodynamics of alternate bars in a channelized, regulated river: An integrated historical and modelling analysis. *Earth Surface Processes and Landforms*, *43*(9), 1739–1756. https://doi.org/10.1002/esp.4349

Siviglia, A., Stecca, G., Vanzo, D., Zolezzi, G., Toro, E. F., & Tubino, M. (2013). Numerical modelling of two-dimensional morphodynamics with applications to river bars and bifurcations. *Advances in Water Resources*, *52*, 243–260. https://doi.org/10.1016/j.advwatres.2012.11.010

Sukegawa, N. (1971). *Study on meandering of streams in straight channels* (pp. 335–363). Japan: Report of Bureau of Resourcess, Department of Science and Technology.

Surian, N., Mao, L., Giacomin, M., & Ziliani, L. (2009). Morphological effects of different channel-forming discharges in a gravel-bed river. *Earth Surface Processes and Landforms*, *34*(8), 1093–1107. https://doi.org/10.1002/esp.1798

Tubino, M. (1991). Growth of alternate bars in unsteady flow. *Water Resources Research*, *27*(1), 37–52. https://doi.org/10.1029/90WR01699

Tubino, M., Repetto, R., & Zolezzi, G. (1999). Free bars in rivers. *Journal of Hydraulic Research*, *37*(6), 759–775. https://doi.org/10.1080/00221689909498510

Vautier, F. (2000). *Dynamique geomorphologique et végétalisation des cours d'eau endigues: l'exemple de l'Isère dans le Grésivaudan*. Grenoble: Université Joseph Fourier.

Vianello, A., & D'Agostino, V. (2007). Bankfull width and morphological units in an alpine stream of the dolomites (Northern Italy). *Geomorphology*, *83*(3–4), 266–281. https://doi.org/10.1016/j.geomorph.2006.02.023

Welford, M. R. (1994). A field test of Tubino's (1991) model of alternate bar formation. *Earth Surface Processes and Landforms*, *19*(4), 287–297. https://doi.org/10.1002/esp.3290190402

Wilcock, P. R., & DeTemple, B. T. (2005). Persistence of armor layers in gravel-bed streams. *Geophysical Research Letters*, *32*(8), L08402. https://doi.org/10.1029/2004GL021772

Williams, G. P. (1978). Bank-full discharge of rivers. *Water Resources Research*, *14*(6), 1141–1154. https://doi.org/10.1029/WR014i006p01141

Wolman, G. M., & Miller, J. P. (1960). Magnitude and frequency of forces in geomorphic processes. *The Journal of Geology*, *68*(1), 54–74. https://doi.org/10.1086/626637